CHAPTER III

NA-A (LTA) ZEOLITE SYNTHESIS DIRECTLY FROM ALUMATRANE AND SILATRANE BY SOL-GEL PROCESS AND MICROWAVE TECHNIQUE

(Journal of European Ceramic Society, In Press)

3.1 Abstract

1 μm crystal size Na-A zeolite was successfully synthesized via sol-gel process and microwave heating technique using alumatrane and silatrane as precursors. After fixing SiO_2:Al_2O_3 ratio at 1:1 and microwave heating temperature at 110°C, increasing the Na_2O concentration by adding more NaOH exponentially reduces the microwave heating time from 160 min at Na_2O:SiO_2 ratio of 3:1 to 5 min at Na_2O:SiO_2 ratio of 9:1. The increase of Na_2O concentration strongly affects the particle size and particle size distribution, but does not affect the product composition. Small crystallite sizes are obtained from high Na_2O:SiO_2 ratio (10:1) while low Na_2O:SiO_2 ratio (3:1) gives large crystallite size (~4.5 μm). The analyzed Si:Al:Na ratio of synthesized Na-A zeolite is 1:1:1.25. The moisture absorption ability of the synthesized Na-A zeolite is higher than that of the commercial one by approximately 20%. The increase of water ratio also affects the crystal size. As the water ratio increases, larger crystallites with a higher degree of irregularity are formed.

Keywords: Alumatrane, Silatrane, Microwave technique, Sol-gel process, and Zeolite A

3.2 Introduction

Zeolites are versatile materials, which are used in many applications, such as household products, aquaculture, agriculture, water treatment, etc. due to their absorption, ion exchange and size selectivity prperties[1]. Na-A zeolite has also been employed in gas separation membranes, to enhance the selectivity of the support[2]. Commercial Na-A zeolite is synthesized by both conventional and microwave heating techniques and mostly silicates and aluminates are used as starting materials.

A Na-A zeolite membrane was produced on αAl_2O_3 support by dipping the support into the gel and then crystallizing the gel by hydrothermal heating at 90°C[3]. The results indicated that microwave heating provided more uniform and small particles with a shorter heating time (4-12 times shorter than conventional heating) and gave four times higher gas permeability with equal selectivity in permeation. A second technique of making Na-A zeolite membrane is to seed the support with Na-A zeolite crystals followed by an one-time-only hydrothermal synthesis at 100°C. The seeding method yielded a dense inter-grown zeolite crystal layer of about 30 μm in thickness on the outer surface[4]. The resulting membranes were highly permeable to water vapor but impermeable to other gases unless dried completely. They exibited excellent water perm-selective performance in water/organic liquid mixtures. The microwave heating times can be shortened by increasing the heating temperature to 100°C. Additionally by increasing the Na_2O concentration, the heating time can be reduced to 5 min[5]. However, the resulting particles had knotted edges due to the fact that pre-nuclei were formed during aging. It was also found that the aging time strongly influences the crystallization time, particle size and yield. Ultrasound and XRD revealed that an amorphous gel is first observed before nucleation and crystallite growth[6]. A similar observation was made by using dynamic light scattering (DLS) to follow zeolite synthesis[7].

Eventhough Na-A zeolite synthesis has been studied in great detail, it is still a challenge to find a new synthetic route, which results in better crystallinity. The use of small amines, such as ethylamine, isopropylamine or diethylamine (short or long primary or secondary amine) as a pore-filler during the crystallization stage,

has been successful in siliceous zeolite synthesis and in controlling the framework structures[8-9]. However, the obtained product contained charge-balancing protonated amine (despite a gel pH often above 13) and had a Na/Al ratio substantially below unity (Na/Al < 1). Our previous work used atranes (metal alkoxides), see Figure 1, as precursors for ANa-And GIS zeolite synthesis via the sol-gel process and resulted in thermodynamically stable materials in an aqueous-base system[10]. Atrane is an amine-trialkoxo complex (with a diversity of elements), in which tertiary amine acts as anionic (tetradetate) tripod ligand and a neutral nitrogen-donor while trialkoxo groups function as polyalcohols making it capable in acting as reagent in sol-gel process[11-17]. These properties increase the possibility of expanding its coordination sphere of inorganic-organic micelle formation during the sol-gel process and hydrothermal treatment. Nevertheless, they moderate the alkoxide reactivity towards the nucleophilic attack of water, resulting in slow precipitation of crystal and nuclei[13, 18-19]. This paper reports further results of our studies on the synthesis of Na-A or LTA zeolite by using the same method with the expectation of a higher uniform crystallinity and a narrower particle size distribution.

3.3 Experimental

3.3.1 Materials

Fumed silica (SiO_2, surface area 474 m^2/g, average particle size of 0.007 μm) and aluminum hydroxide hydrate ($Al(OH)_3$, surface area 51 m^2/g), were purchased from Sigma Chemical Co. and used as received. Triethanolamine (TEA, $N(CH_2CH_2OH)_3$), and triisopopanolamine (TIS, $N(CH_2CHCH_3OH)_3$) were supplied by Carlo Erba Reagenti and Fluka Chemical AG., respectively, and used as received. Ethylene glycol (EG, $HOCH_2CH_2OH$) was obtained from J.T. Baker Inc. and distilled using fractional distillation prior to use. Sodium hydroxide (NaOH) and sodium chloride (NaCl) were purchased from EKA Chemicals and AJAX Chemicals, respectively. Both were used as received. Acetonitrile (CH_3CN) was obtained from Lab-Scan Co., Ltd. and distilled using standard purification methods prior to use.

3.3.2 Instrumentals

FTIR spectroscopic analysis was conducted using Bruker Instrument (EQUINOX55) with a resolution of 4 cm^{-1} to measure functional groups of materials. The solid samples were prepared by mixing 1% of sample with dried KBr, while the liquid samples were analyzed using Zn-Se window cell. For the measuring of the molar mass of precursors, mass spectra were obtained by means of a VG Autospec model 7070E from Fison Instruments with VG data system, using the positive fast atomic bombardment (FAB^+-MS) mode and glycerol as a matrix. CsI was used as a reference, while a cesium gun was used as an initiator. The mass range used was from m/e = 20 to 3,000. Thermal properties and stability were analyzed by thermogravimetric analysis (TGA) and differential scanning calorimetry (DSC). TGA was performed using a Perkin Elmer TGA7 analyzer while DSC was conducted with a Netzsch instrument: DSC200 Cell at a heating rate of 10°C/min under nitrogen atmosphere. Aluminum pans containing 5 – 10 mg of sample were used in DSC analysis, while a platinum pan containing 10 – 20 mg of sample was used in TGA. For the liquid and gel samples, a high-pressure gold cell containing 10-20 mg of sample was used. The crystallinity of products were characterized by Rigaku X-Ray Diffractometer at a scanning speed of 5 degree/sec using CuKα as a source and CuKβ as a filter. XRD spectra were recorded after theta/2 theta scans in the range 5 – 50°. SEM micrographs were obtained with a JEOL 5200-2AE scanning electron microscope. Electron Probe Microanalysis (EPMA) was used for both qualitative and quantitative elemental analysis using the X-Ray mode detector (SEM/EDS) to obtain product compositions. Particle sizes and particle size distributions were determined by using Malvern Instruments Mastersize X Ver.2.15 analyzer. Water was used as a mobile phase. Hydrothermal treatment by microwave heating technique was conducted using MSP1000, CME Corporation (Spec. 1,000W and 2,450 MHz). Samples were heated in a Teflon-lined digestion vessel using inorganic digestion mode with time-to-temperature program.

3.3.3 Precursor Synthesis

Silatrane synthesis was performed by mixing silicon dioxide, 0.10 mol, and triethanolamine, 0.125 mol, in a simple distillation set using 100 ml of ethylene glycol, as solvent[20]. The reaction was carried out at the boiling point of ethylene glycol under nitrogen flowing to remove the by-product water and ethylene glycol from the system. The reaction was carried out for 10 h and the rest of ethylene glycol was removed under vacuum (10^{-2} torr) at 110°C for 8 h. The brownish white solid was washed three times with dried acetonitrile (or untill the filtrate had no color) to remove undesired organic residues. Approximately 95% yield white powder product was obtained and characterized using FTIR, TGA, DSC and FAB^+-MS.

A similar process was used to synthesize alumatrane from aluminum hydroxide (0.1 mol) and triisopropanolamine (0.125 mol)[21]. The crude product was washed with dried acetonitrile for three times to give approximately 90% yield of the final product, which was characterized using FTIR, TGA, DSC and FAB^+-MS.

3.3.4 Sol-Gel Process and Microwave Technique

SiTEA and AlTIS were mixed with NaOH or NaCl solution at room temperature at a ratio of SiO_2:Al_2O_3:xNa_2O:yH_2O (where $0 \leq x \leq 10$ and $63 \leq y \leq 1000$). The solution mixture was aged for at least 12 h to obtain fully gel formation and then placed into a Teflon vessel for further hydrothermal treatment using the microwave technique. The solution mixtures containing different ratios of SiO_2:Al_2O_3: xNa_2O:yH_2O were treated for various time and the resulting white powder products were washed three times using distilled water. The products were finally dried at 75°C for 15 h prior to characterization using DSC/TGA, FTIR, XRD, N_2 porosimetry (BET is the analysis method) and SEM.

3.3.5 Moisture Absorption

Crucibles were heated at 350°C for 10 h. and cooled to 120°C in a hot-air oven. They were then moved and kept in a dessicator until use. The samples and the dried crucibles were weighed and then heated at 350°C for 10 h. They were

cooled to 120°C in oven and then kept in dessicator until they cooled to room temperature. The dried samples were weighed and dried weight of sample (W_1) was calculated. The dried samples were placed in a closed humidification chamber for 15 h. and then weighed to determine the mass of water adsorbed (W_2). The moisture absorption ability was calculated per unit mass of the sample (W_2/W_1).

3.4 Results and Discussion

3.4.1 Precursor Synthesis

Via the Oxide-One-Pot-Synthesis (OOPS) process, silatrane and alumatrane were successfully synthesized directly from silica and alumina. Due to the condensation reaction generating water as a byproduct, the reactions were carried out under a nitrogen atmosphere and water was removed from the system to drive the reactions forward. The products can slowly absorb moisture and then undergo hydrolysis process, thus need to be kept under vacuum.

The FTIR spectrum of the synthesized alumatrane shows the following significant peaks: 2860-2986 cm^{-1} (m, νC-H), 1244-1275 cm^{-1} (m, νC-N), 1130 cm^{-1} (m, νC-O), 1102 cm^{-1} (s, νAl-O-C), 1037 cm^{-1} (m, νC-O), 890 cm^{-1} (s, δ Al-O-C) and 649-400 cm^{-1} (s, δAl-O). The TGA results give two mass loss transitions at 139° and 393°C with 24% ceramic yield corresponding to the structure of $Al(OCHCH_3CH_2)_3N$, which has 23.7% theoretical ceramic yield. Coincidentally, DSC also shows 145°C (endothermic) and 380°C (exothermic) referring to decomposition of organic ligand and oxidation of carbon residue, respectively, since a second heating cycle (after the first heat-cool cycle) revealed no endothermic transition as the material had undergone degradation. The other method to confirm the structure of the desired product is FAB^+-MS giving the base peak at m/e 216 belonging to the structure of $Al(OCHCH_3CH_2)_3\ NH^+$ and approximately 5% of the molecular peak at m/e 1292, which belongs to $(Al(OCHCH_3CH_2)_3N)_6H^+$.

Concerning the synthesized silatrane product, its FTIR spectrum showed the following peaks: 3000-3700 cm^{-1} (w, νO-H), 2860-2986 cm^{-1} (s, νC-H), 1244-1275 cm^{-1} (m, νC-N), 1170-1117 cm^{-1} (bs, νSi-O), 1093 cm^{-1} (s, νSi-O-C),

1073 cm^{-1} (s, νC-O), 1049 cm^{-1} (s, νSi-O), 1021 cm^{-1} (s, νC-O), 915 - 940 cm^{-1} (m, δSi-O-C), 785 and 729 cm^{-1} (s, δSi-O-C) and 579 cm^{-1} (w, Si<---N). In this case, TGA thermogram provides only one mass loss transition at 390°C with 18.5 %ceramic yield corresponding to $Si((OCH_2CH_2)_3N)_2H_2$, whose theoretical ceramic yield is 18.6%. DSC thermogram shows two peaks at 349°C (endothermic) and 373°C (exothermic). Again, these two peaks are attributed to the decomposition of the organic ligand and oxidation of the carbon residue, respectively. FAB^+-MS gives the molecular as well as base peak at m/e 323 of $Si((OCH_2CH_2)_3N)_2H_3^+$.

3.4.2 Sol-Gel Process

The hydrolytic reaction of the silatrane and alumatrane mixture in NaOH or $NaCl/H_2O$ solution was followed by FTIR, as shown in Figure 2. The NaOH system showed significant change at the Si-O-C and Al-O-C regions, 1000-1170 cm^{-1}. The peak at 1049 cm^{-1} referring to Si-O-Si was higher and broader, while the peak at 1102 cm^{-1} corresponding to Al-O-Al was slightly shifted to higher frequency and became broader. The C-O-M, M = Si or Al, peak at 1021 cm^{-1} was also reduced due to the cleavage of the organic ligand from the system. This was confirmed by the reduction of C-N peak at 1275 cm^{-1} by curve fitting of the area under the peak. The approximate rate of hydrolysis during the sol-gel process was determined from Figure 3. As can be seen in this figure, the hydrolysis rate was two times faster with hydroxyl anion (OH^-). The hydroxyl ion attacked Si- or Al-atom faster and easier to form hydroxide in the hydrolysis step due to the lower electronegativity of M-Cl bond and the weaker nucleophilicity of Cl^- [22]. The hydroxyl group of metal hydroxide part attacked Si- or Al-atom of other groups to form metal-oxygen-metal bridge and the organic part was released in the condensation step. With both anions, OH^- and Cl^-, the hydrolysis rate was rapid during the first hour and then became much slower.

3.4.3 Gel Transformation to Aluminosilicate

Both alumatrane and silatrane underwent hydrolysis and condensation reactions in a system of NaCl/water or NaOH to form amorphous

metal oxide gel. The amorphous gel was aged for 12-15 h to obtain complete gelation. The gel was transformed to a crystalline aluminosilicate by hydrothermal treatment using the microwave-heating technique. The nucleation occurred first at this step and was followed by the formation of the crystalline product. We found that the gel started to form at the SiO_2:Na_2O ratio of 1:0.0069 and the ratios of SiO_2:Na_2O to start with the synthesis of LTA were in the range of 1:3 to 1:10. The amount of water started from y = 410 to y = 510 due to the homogeneous dispersion of the powder product in solution mixture and the suitable SiO_2:H_2O ratio for synthesizing LTA was 1:410. By fixing the ratio of starting materials SiO_2:Al_2O_3:xNa_2O:yH_2O at 1:1:3:410 and the microwave heating temperature at 110°C for 3 h, XRD results indicated that only the NaOH/H_2O system can provide crystalline aluminosilicate, as illustrated in Figure 4. The XRD results were matched with the Linde (A-LTA) structure having PDF# 39-0222 and $Na_{96}Al_{96}Si_{96}O_{384}.216H_2O$ ~ Si:Al:Na = 1:1:1. SEM confirmed (Figure 5) that the building unit was in cubic form, developed from the connection of sodalite cage (β-cage or T24 unit) along the cube axes through double T4-rings. The crystallographic data are listed in Table 1. Moreover, the EDS-SEM results showed that the synthesized product contained only Si-, Al- and Na-Atoms, and the ratio of Si:Al:Na ratio was 1:1:1.25 due to the interaction of OH^- anions with the zeolite framework in order to form the siloxy groups ($\equiv SiO^-$), which must be accommodated with extra Na^+ cations[23]. The TGA and DSC results of synthesized zeolite also indicated no mass loss of residue carbon and no phase-transformation in the range of 150°–600 ° C. The thermal stability limit of the synthesized product was 600 °C. XRD results also indicated the same phenomeNa-As those obtained from TGA and DSC. Even at 700 °C LTA was found as a major product. The baseline was changed to curve and the signal to noise ratio was higher indicating the morphology change of LTA (Figure 6).

By following the reaction using XRD, the amorphous gel was firstly transformed to crystalline aluminosilicate at 60 min. and the transformation was complete at 160 min, as illustrated in Figures 7 and 8. The SEM micrographs also show the same results as the XRD spectra, and the Na-A zeolite was started to form

at microwave heating time of 60 min. The observed Na-A zeolite was in a sharp edge cubic shape which indicated that pre-nuclei might not be formed due to the organic-inorganic micelle formation during the sol-gel process[18, 24-28]. The complex formation not only prevented the precipitation to occur, but also retarded the nucleophilic attack of water, which enhanced the metal-oxide-metal formation (condensation reaction), allowing three-dimensional network to form. Additionally, the formation of complexes also helped dissolving amorphous aluminosilicate gel and slowly precipitating crystalline aluminosilicate resulting in the low defect crystallization. However, we also observed some irregular cubic crystallites of Na-A zeolite, most likely due to the growing of new nuclei after the initial nucleation and precipitation. The Si/Al ratio of the synthesized products versus microwave heating time was reduced from 1.53 to ~1.00, as shown in Figure 9. Even when we used Si/Al ratio less than 1, some aluminum became sodium aluminate dissolved in NaOH solution. The Si/Al ratio dropped significantly at 140 min at which almost all of the crystalline products was formed. This is confirmed by the SEM results (Figure 8). After crystalline formation, the Si/Al ratio approached unity while the Na/Al ratio was greater than one (~1.25).

3.4.4 Effect of NaOH Concentration

In previous paper[10], we had reported that Na_2O concentration and temperature affected the microwave heating time. In this work, the source of Na_2O is NaOH, and thus the use of more Na_2O implies increased OH^- concentration (OH^-/SiO_2 ratio = 2(Na_2O/SiO_2 ratio)). In this investigation, we fixed the microwave heating temperature at 110°C and the ratio of SiO_2:Al_2O_3:410H_2O. The Na_2O/SiO_2 concentration ratio was varied from 3 to 10. It was found that as the Na_2O concentration increased, the microwave heating time was reduced dramatically in the range of Na_2O:SiO_2 ratio from 3:1 to 5:1, as illustrated in Figure 10. We speculate that this is due to the fact that the increase in Na_2O concentration increased the hydroxyl concentration, which in turn enhanced the dissolving rate of amorphous gel and the nucleation rate leading to the growth of more crystals. At Na_2O:SiO_2 ratios higher than 5:1, the reaction time decreased slightly and at the Na_2O:SiO_2 ratios of 9:1 and 10:1, the microwave heating time was reduced to 5 min. However,

high concentration of Na_2O did affect the particle size and particle size distribution, as shown in Figure 11. For $Na_2O:SiO_2$ ratios of 3:1 to 5:1, the particle size distribution was bimodal with peaks at 2.16 and 7.84 μm, respectively. As the $Na_2O:SiO_2$ ratio increased to 6:1 and 7:1, the average particle size of each modal was shifted to lower, 1.62 and 7.08 μm, respectively, whereas at $Na_2O:SiO_2$ ratios higher than 7:1, the particle size distribution was changed to mono-modal with smaller particle size (less than 4 μm). For $Na_2O:SiO_2$ ratios equal to 9:1 and 10:1, the particle size distributions were the same. However, from SEM results (Figure 12), the crystal size was different. It was found that the crystals agglomerated due to the presence of much more nuclei in the system. As compared to the $Na_2O:SiO_2$ ratio of 3:1, the average crystal size was ~ 4.5 μm which was half of the result obtained from the particle size analyzer. Obviously, the particles tented to agglomerate more than be freeform. Moreover, increasing the Na_2O concentration did not affect the product composition. All synthesized Na-A zeolites have the Si:Al:Na ratio of ~1:1:1.25.

Since the Na_2O concentration and hydroxyl group concentration were proportional, when increasing the Na_2O concentration, the HO^- concentration increased as well, introducing thus higher pH for the system. When the pH was fixed by controlling the OH^- loading, and adding NaCl to increase the Na_2O concentration was the same with the syntheses carried out under the same OH^- concentration, implying that the major influence on crystalline formation was OH^- concentration.

3.4.5 Effect of Water Quantity

Upon increasing the amount of water from 410 to 510 at the $SiO_2:Al_2O_3:10Na_2O$ ratio and using a microwave heating temperature of 110°C for 5 min, the agglomerate particle size distribution of synthesized Na-A zeolite was almost the same. However, the results from SEM were slightly different, as shown in Figure 13. Higher water quantity leads to slightly bigger particle sizes (~1.5 μm for 510 H_2O and ~1 μm for 410 H_2O). Moreover, more irregular cubic particles were observed. The reason is that when increasing the amount of water the pressure of hydrothermal system is increased, as a result, accelerating thus the crystallization

process. Higher crystallization rates lead to less time to reach the most thermodynamically favored lattice positions resulting in irregular particle sizes and shapes. By fixing the microwave heating temperature at 110°C and H_2O quantity at 410, we were able to construct the 3-phase diagram, illustrated in Figure 14. This phase diagram was constructed from the loading condition that can provide LTA product. Only Si:Al loading ratio of 1:2 provided the LTA type zeolite. At Si:Al ratio of 1:1, the mixture of LTA and GIS type zeolite were obtained while at 1:3, a mixture of LTA and amorphous alumina was produced. This is attributed to the enhanced formation of octahedral aluminium atoms at high Al-concentration.

3.4.6 Moisture Absorption Testing

Comparing moisture absorption ability of two synthesized zeolites at SiO_2:Al_2O_3:410H_2O ratio and hydrothermal crystallization at 110°C with commercial Na-A zeolite (purchased from Aldrich), the absorption ability of synthesized zeolite was determined to be 1.22 and 1.15 times higher for Na_2O:SiO_2 = 3:1 and 10:1, respectively, than that of commercial Na-A zeolite, as summarized in Table 2. The reason for the better moisture absorption capability of the product synthesized at the Na_2O:SiO_2 ratio of 3:1 might be the lower agglomeration of particles, as can be observed from the SEM results given in Figure 12.

3.5 Conclusions

Na-A zeolite can be synthesized by using alumatrane and silatrane as precursors via the sol-gel process and microwave technique. Due to organic-inorganic micelle formation, the sharp edged crystals were formed indicating a better crystallization. Increased Na_2O concentration (by increasing NaOH) leads to decreased microwave heating times and smaller particle sizes. The shortest microwave heating time was 5 min. when the Na_2O:SiO_2 ratios of 9:1 – 10:1 were used. Moreover, the agglomerated crystals were increased as Na_2O concentration increased while the composition of all synthesized Na-A zeolites was the same (Si:Al:Na ratio of ~1:1:1.25). Increased water quantity influenced the particle size

and number of irregular particles due to the pressure built up in the hydrothermal system, which enhanced the nuclei growth and crystallization rates. The moisture absorption ability of synthesized Na-A zeolite was found to be higher than that of commercial Na-A zeolite.

3.6 Acknowledgement

This research work was fully supported by the Thailand Research Fund (TRF).

3.7 References

1. J. Weitkamp, J. C. Jansen, H. G. Karge, Advanced Zeolite Science and Application, Elsevier Science, 1994, p. 632.
2. H. Yahiro, A. Lund, R. Aasa, N. P. Benetis, M. Shiotani, J. Phys. Chem. A.104 (2000) 7950.
3. a). X. Xiaochun, Y. Weishen, L. Jie, L. Liwu, Adv. Mater. 12 (2000) 195.; b.) Z. Pilter, S. Szabó, M. Hasznos-Nezdei and E. Pallai-Varsányi, Microporous and Mesoporous Materials 40 (2000) 257.; c.) X. Xiaochun, Y. Weishen, L. Jie, L. Liwu, Separation and Purification Technology 25 (2001) 241.
4. O. Ken-ichi, K. Hidetoshi, H. Kohji, T. Kazuhiro, Ind. Eng. Chem. Res. 40 (2001) 163.
5. P.M. Slangen, J.C. Jansen, H. Van Bekkum, Micro. Mat. 9 (1997) 259.
6. M. Schmachtl, T.J. Kim, W. Gill, R. Herrmann, O. Scharf, W. Schwieger, R. Schertlen, C. Stenzel, Ultrasonics 38 (2000) 809.
7. D. Caputo, B. De Gennaro, B. Liguori, F. Resta, L. Carotenuto, C. Piccolo, Mat. Chem. Phys. 66 (2000) 120.
8. L.D. Rollmann, J.L. Schlenker, S.L. Lawton, C.L. Kennedy, G.J. Kennedy, D. Doren, J. Phys. Chem. B. 103 (1999) 7175.
9. L.D. Rollmann, J.L. Schlenker, C.L. Kennedy, G.J. Kennedy, D. Doren, J. Phys. Chem. B. 104 (2000) 721.
10. M. Sathupunya, E. Gulari, and S. Wongkasemjit, J. Eur. Cer. Soc. (submitted).

11. A. Naiini, V. Young, J. Verkade, Polyhedral 14 (1995) 393.
12. H. Brown, E. Flecher, J. Am. Chem. Soc. 73 (1951) 2802.
13. C. Frye, G. Vicent, W. Finzel, J. Am. Chem. Soc. 93 (1971) 6805.
14. F. Hein, P. Albert, Z. Anorg. Allg. Chem. 269 (1952) 67.
15. A. Schleppnik, D. Gustche, J. Am. Chem. Soc. 25 (1960) 1370.
16. M. Voronkov, Pure Appl. Chem. 13 (1966) 35.
17. D. Milbrath, J. Verkade, J. Am. Chem. Soc. 92 (1997) 6607.
18. S. Cabrera, J. E. Haskouri, C. Guillem, J. Latorre, A. Beltran-Porter, D. Beltran-Porter, M. D. Marcos, P. Amoros, Solid State Science 2 (2000) 405.
19. P. E. A. DeMoor, T. P. M. Bcelen, R. A. VanSanten, L. W. Beck, M. E. Davis, J. Phys. Chem. B. 104 (2000) 7600.
20. P. Piboonchaisit, S. Wongkasemjit and R. Laine, Science-Asia, J. Sci. Soc. Thailand 25 (1999) 113.
21. Y. Opornsawad, B. Ksapabutr, S. Wongkasemjit, R. Laine, Eur. Polym. J. 37/9 (2001) 1877.
22. E. M. Rabinovich, Sol-Gel Technology For Thin Filmes, Fibers, Electronic and Specially Shapes, Nayes Publication, New Jersey, 1988, p.
23. V. Shen, K. Watanabe, A. T. Bell, J. Phys. Chem. B. 101 (1997) 2207.
24. C. Kresge, M. Leonowicz, M. Roth, J. Vartuli, J. Beck, Nature 359 (1992) 710.
25. A. Corma, Chem. Rev. 97 (1997) 2373.
26. J. Ying, C. Mehnert, M. Wong, Angew. Chem. Int. Ed. Engl. 38 (1999) 56.
27. A. Monnier, F. Schuth, Q. Huo, D. Kumar, D. Margolese, R. Maxwell, G. Stucky, M. Krishnamurty, P. Petroff, A. Firouzi, J. Janiche, B. Chmelka, Science 261 (1993) 1290.
28. D. Antonelli, J. Ying, Angew. Chem. Int. Ed. Engl. 34 (1995) 2014.

Table 3.1 Results of XRD Analysis

Data Source	Experiment	JCPDS-ICDD
Name	Na A	Na A
Type	A-LTA	A-LTA
Crystal System	Cubic	Cubic
Space Group (SG)	Pm3m	Fm3c
a (Å)	12.25	24.61
b (Å)	12.25	24.61
c (Å)	12.25	24.61
Unit Cell Volume ($Å^3$)	1838.27	14905.10
λ (Cu-Kα) (Å)	1.54056	1.5418
Filter	Cu-Kβ	
Data Collection Range (2θ, deg.)	5 – 50	
Data Collection Instrument	Rigaku X-Ray Diffractometer	
Matched PDF#	39-0222	

Table 3.2 Moisture absorption of synthesized zeolites at SiO_2:Al_2O_3:xNa_2O: 410H_2O (x = 3 and 10) and 110°C as compared with commercial zeolite (purchased form Aldrich)

Condition	Water Absorption (gH_2O/g)	Ratio
$Na_2O/SiO_2 = 3$	0.1598	1.216
$Na_2O/SiO_2 = 10$	0.1508	1.148
Commercial Zeolite	0.1314	1.000

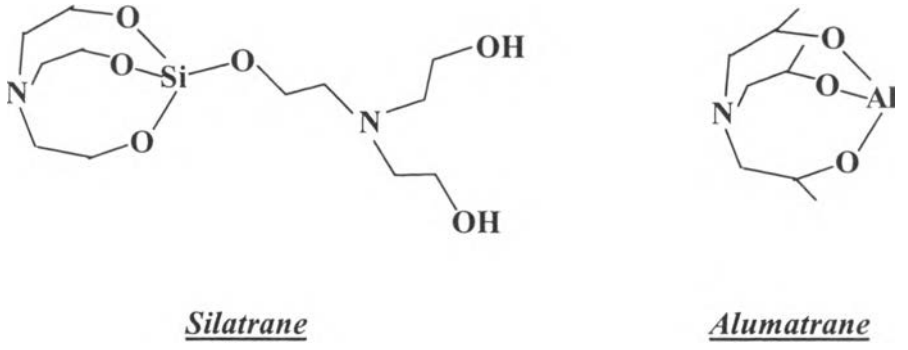

Silatrane ***Alumatrane***

Figure 3.1 The structures of synthesized silatrane and alumatrane

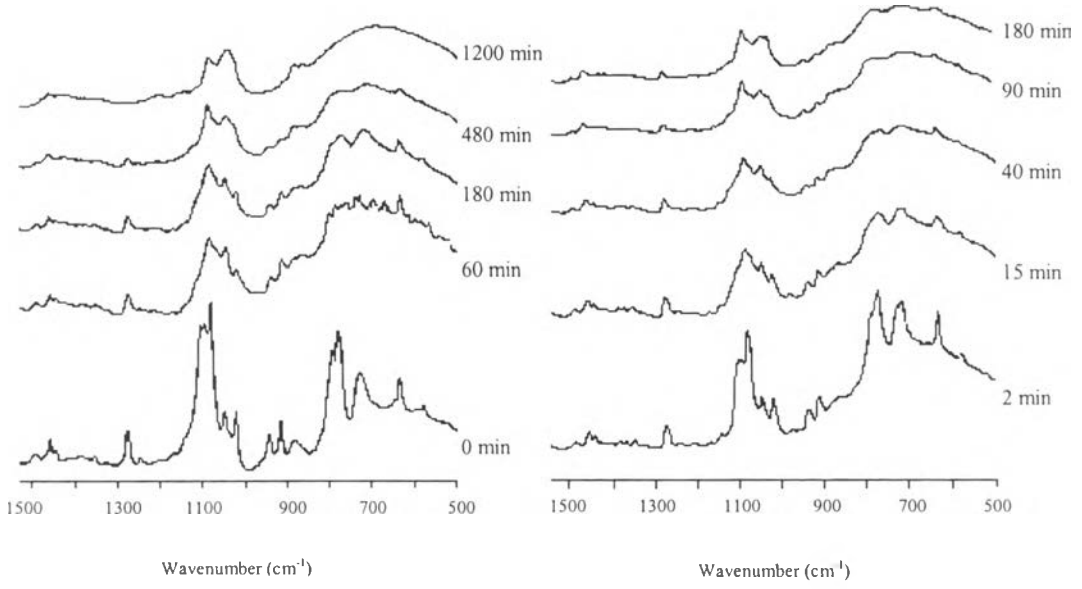

(a) (b)

Figure 3.2 Hydrolysis behavior of alumatrane and silatrane mixture at the ratio of $1SiO_2$:$0.5Al_2O_3$:$0.096Na_2O$:$63H_2O$ in (a) $NaCl/H_2O$ and (b) $NaOH/H_2O$ system

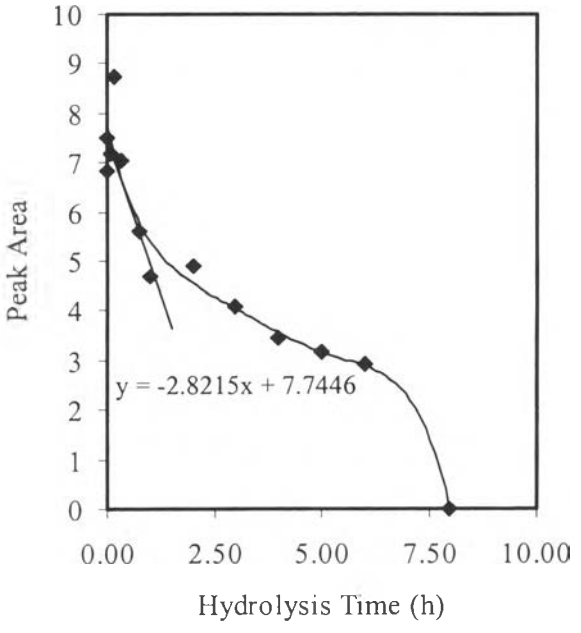

(a)

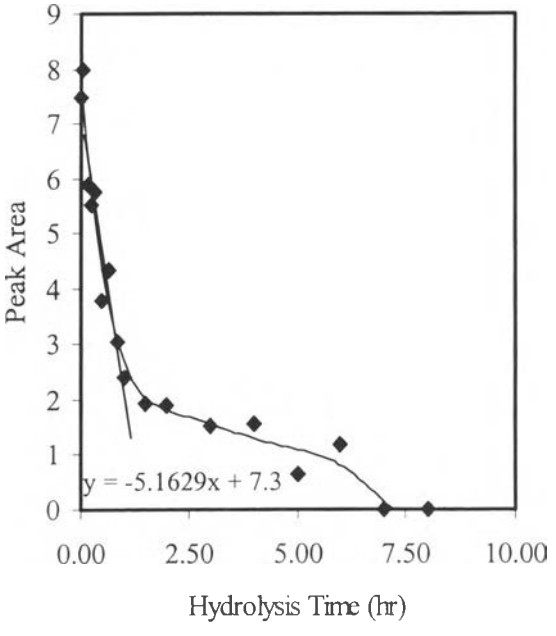

(b)

Figure 3.3 Reduction rate of νC-N peak at 1275 cm^{-1} of the mixture containing $1SiO_2:0.5Al_2O_3:0.096Na_2O:63H_2O$ in (a) $NaCl/H_2O$ and (b) $NaOH/H_2O$ system

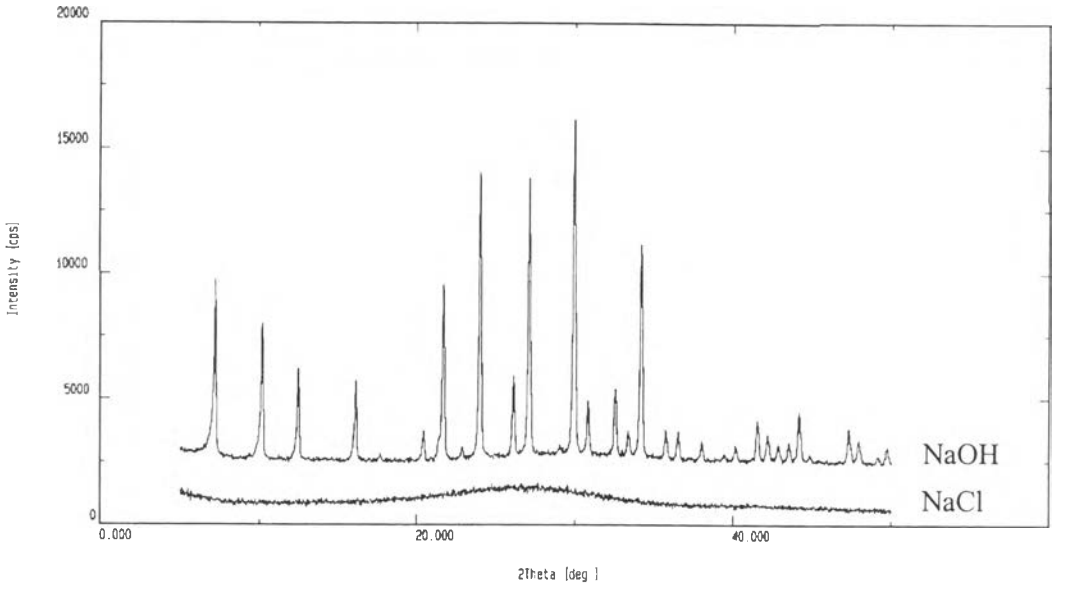

Figure 3.4 XRD spectra of aluminosilicate synthesized from SiO_2:Al_2O_3:3Na_2O: 410H_2O and 110°C for 180 min in NaCl/H_2O and NaOH/H_2O system

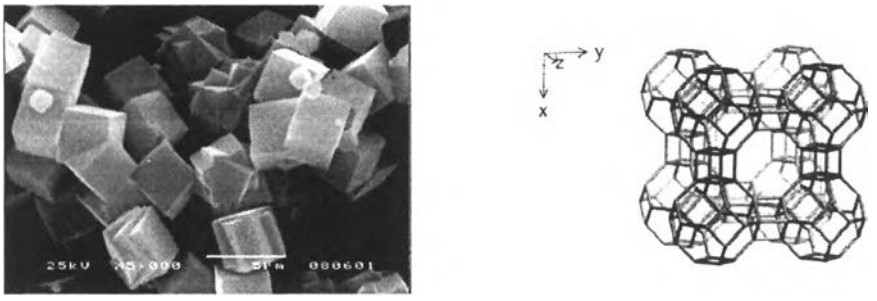

Figure 3.5 Unit cell structure and crystal morphology of Na A zeolite synthesized from SiO_2:Al_2O_3:$3Na_2O$:$410H_2O$ and 110°C for 180 min in $NaOH/H_2O$ system

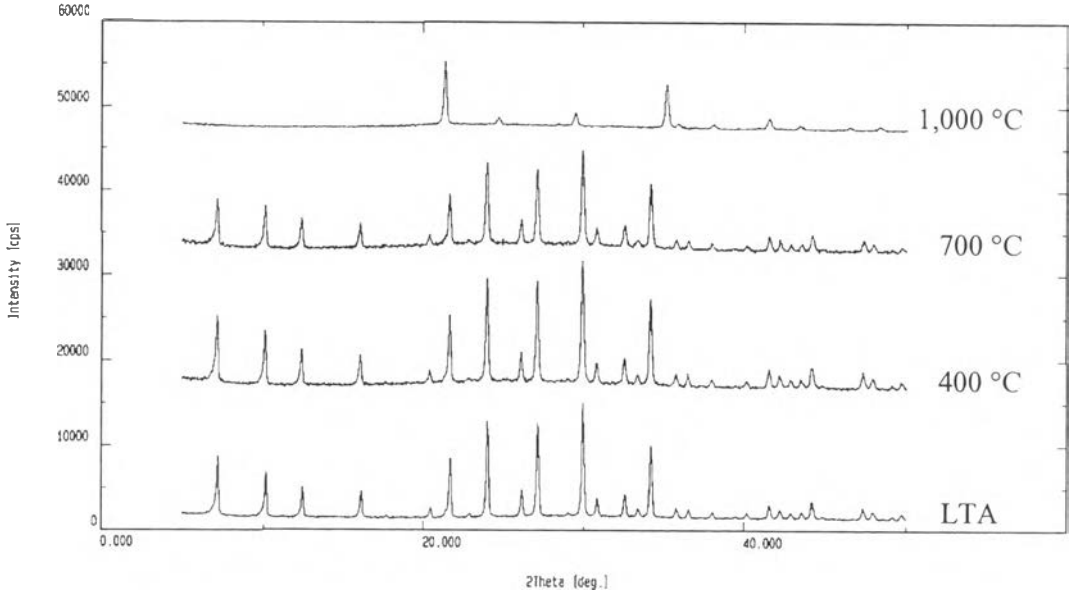

Figure 3.6 XRD spectra of calcinated Na A zeolite at various temperature (room temperature to 1000 °C)

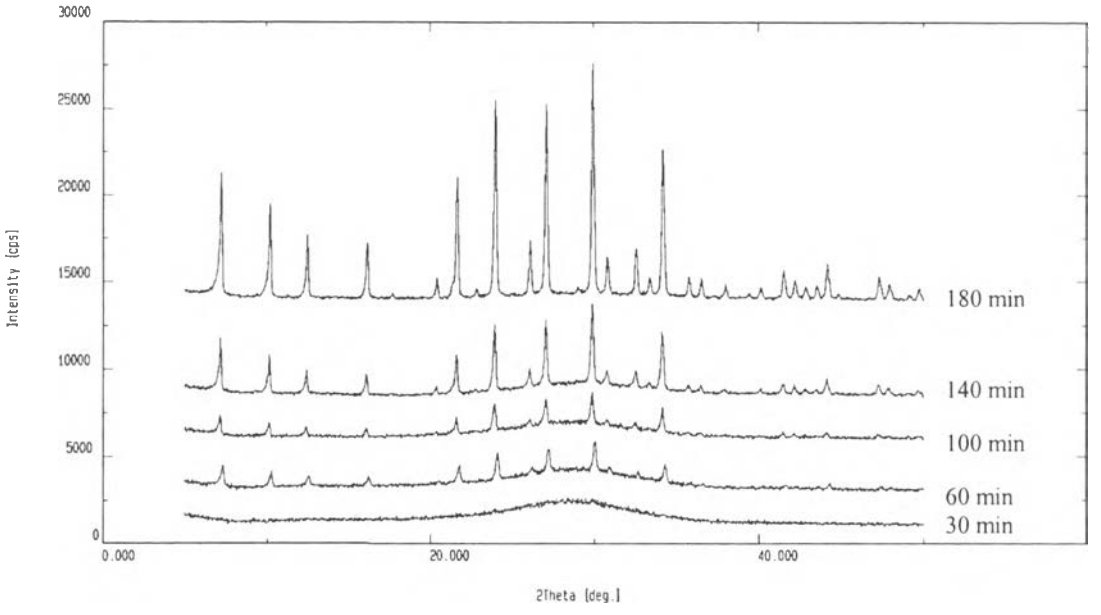

Figure 3.7 XRD spectra of Na A zeolite synthesized from SiO_2:Al_2O_3:3Na_2O: 410H_2O and 110°C for x min (x = 30 – 180 min)

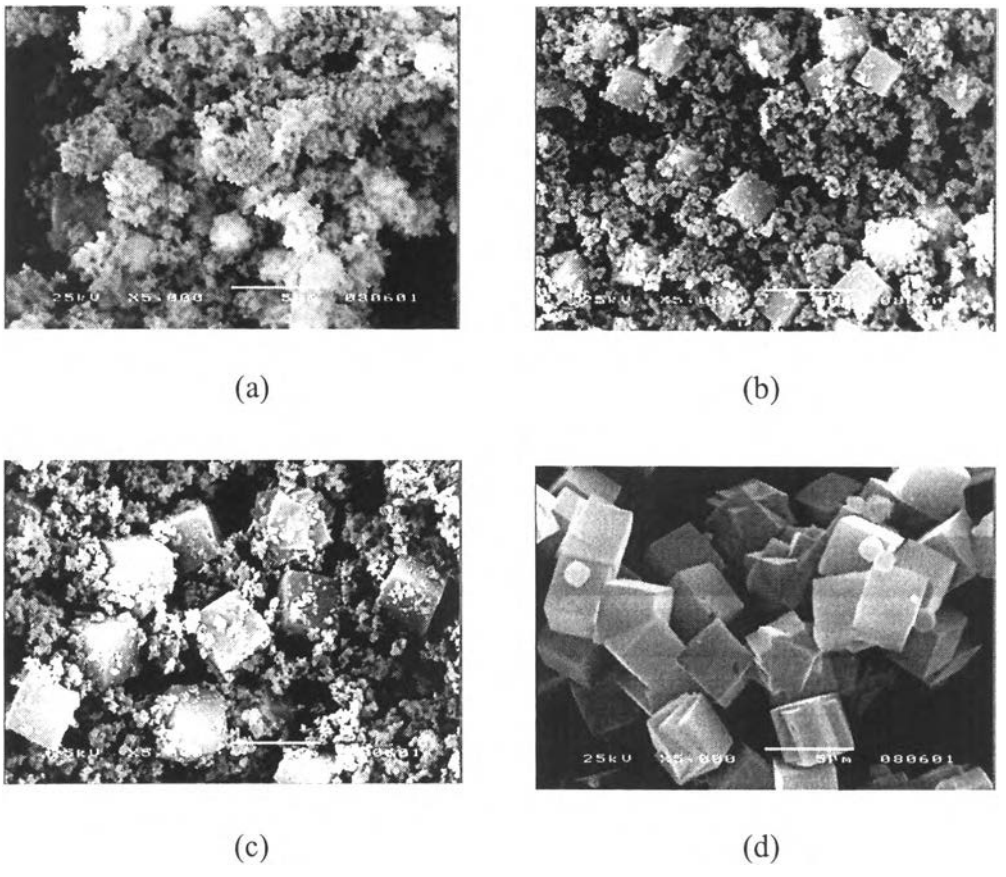

Figure 3.8 SEM micrographs of Na A zeolite synthesized from SiO_2:Al_2O_3: $3Na_2O$: $410H_2O$ and 110°C for (a) 60, (b) 100, (c) 140 and (d) 160 min

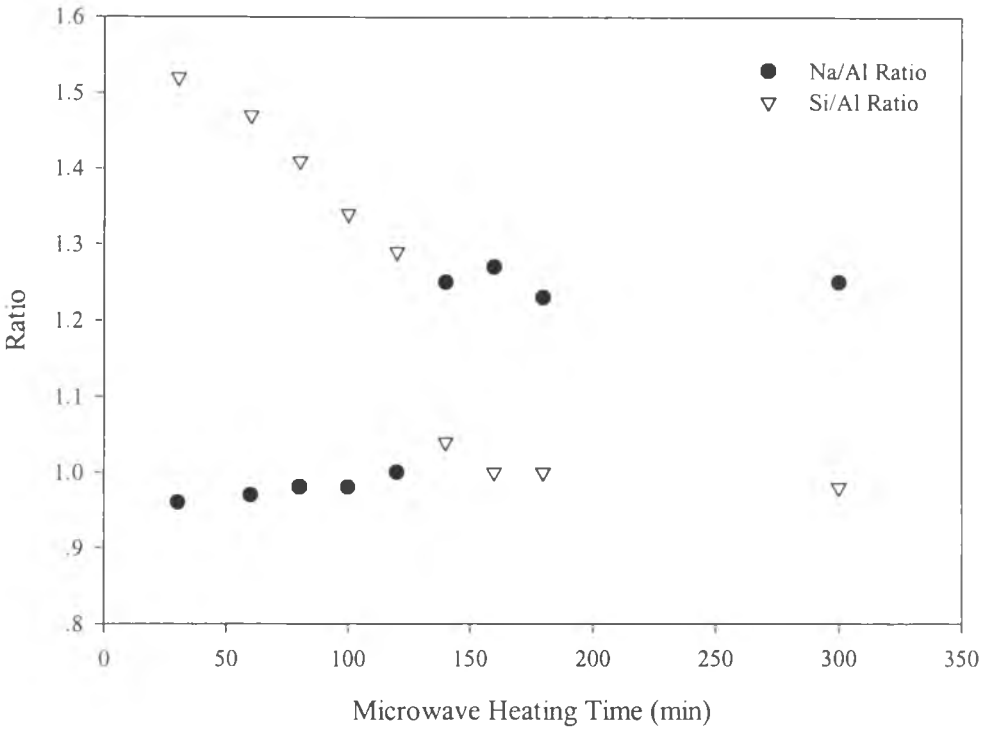

Figure 3.9 Na/Al and Si/Al ratios of synthesized zeolites at SiO_2:Al_2O_3:3Na_2O: 410H_2O and 110°C for x min (30 – 180 min)

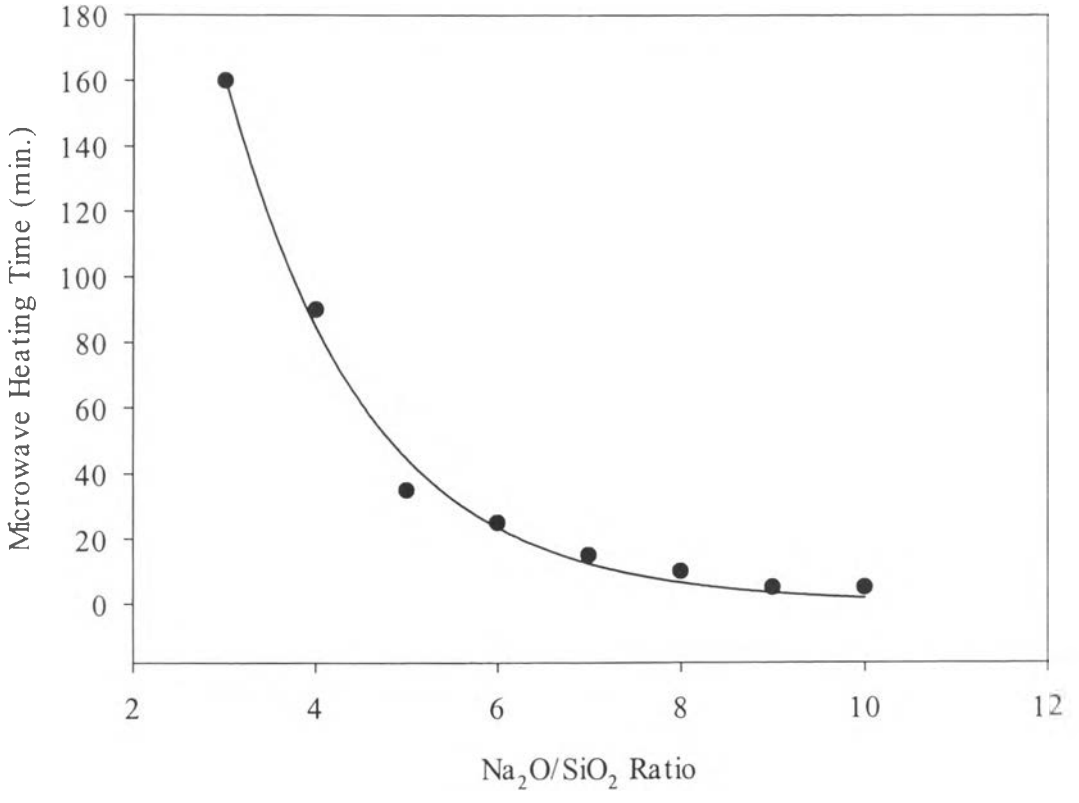

Figure 3.10 Effect of NaOH concentration on Na A zeolite synthesis using SiO_2:Al_2O_3: xNa_2O:$410H_2O$ (x = 3 - 10) and 110°C

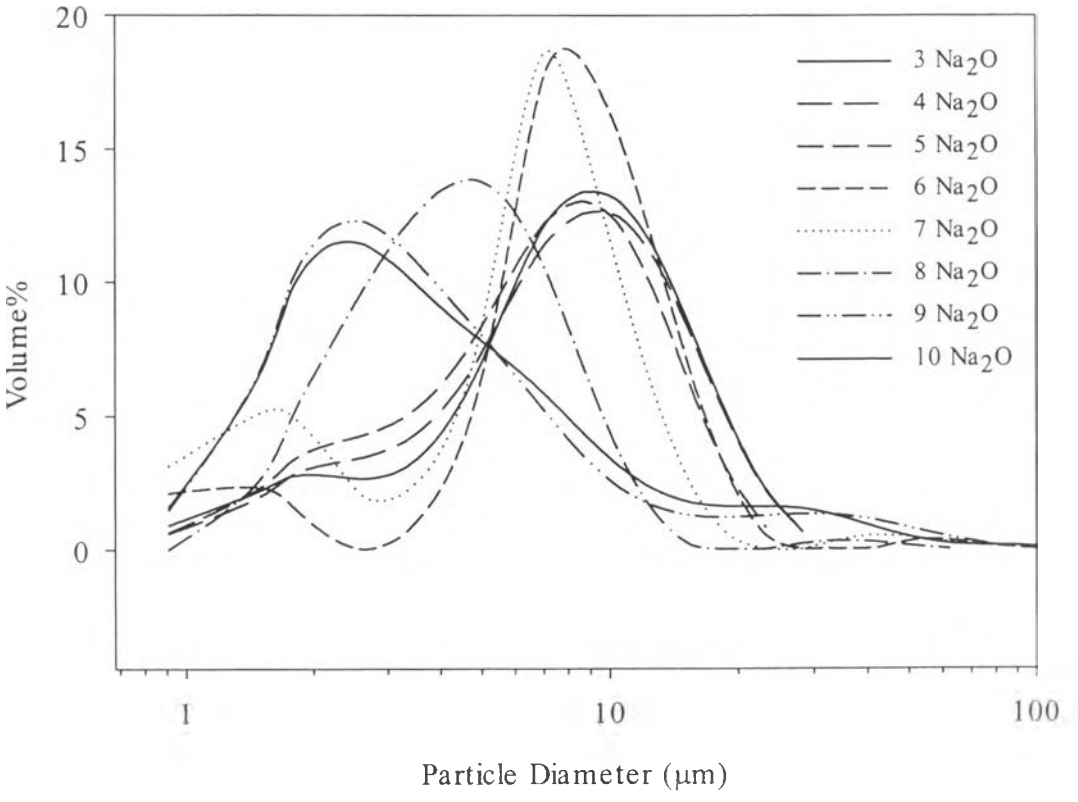

Figure 3.11 Agglomerated particle size distribution of Na A zeolite synthesized at various Na_2O concentration at SiO_2:Al_2O_3:xNa_2O:410H_2O (x = 3 - 10) and 110° C/180 min

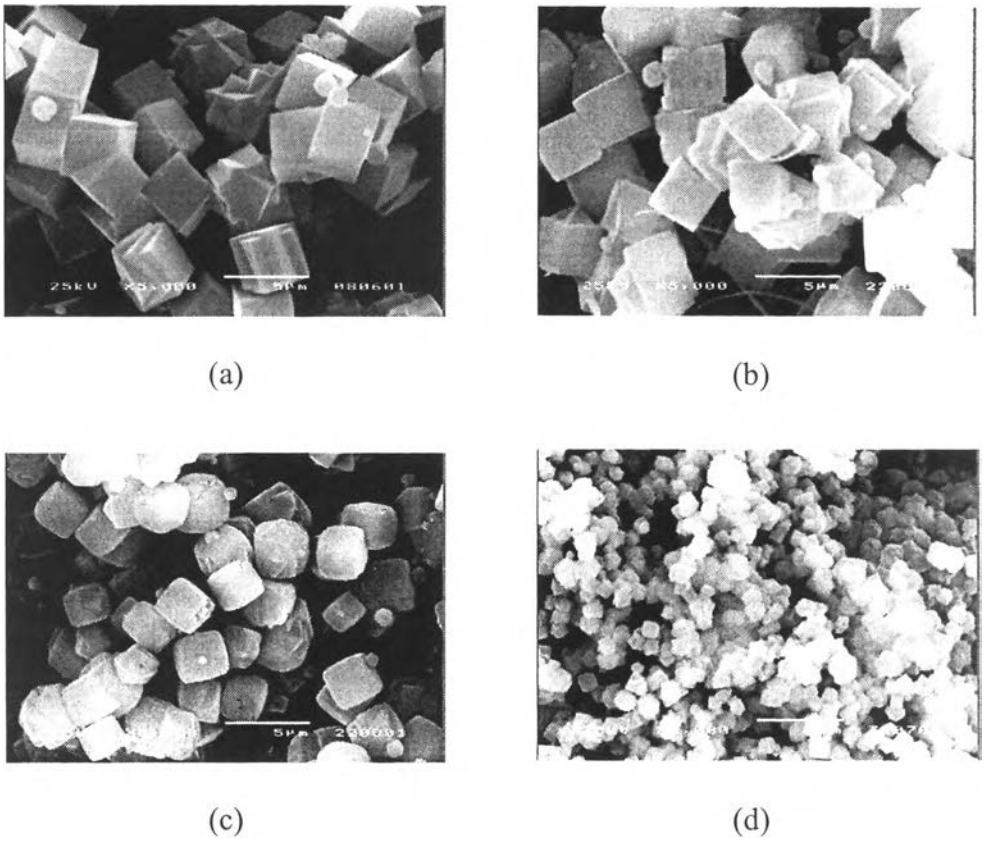

Figure 3.12 SEM micrographs of Na A zeolite synthesized using SiO_2:Al_2O_3: xNa_2O: 410H_2O and 110°C, with x = (a) 3, (b) 7, (c) 8 and (d) 10

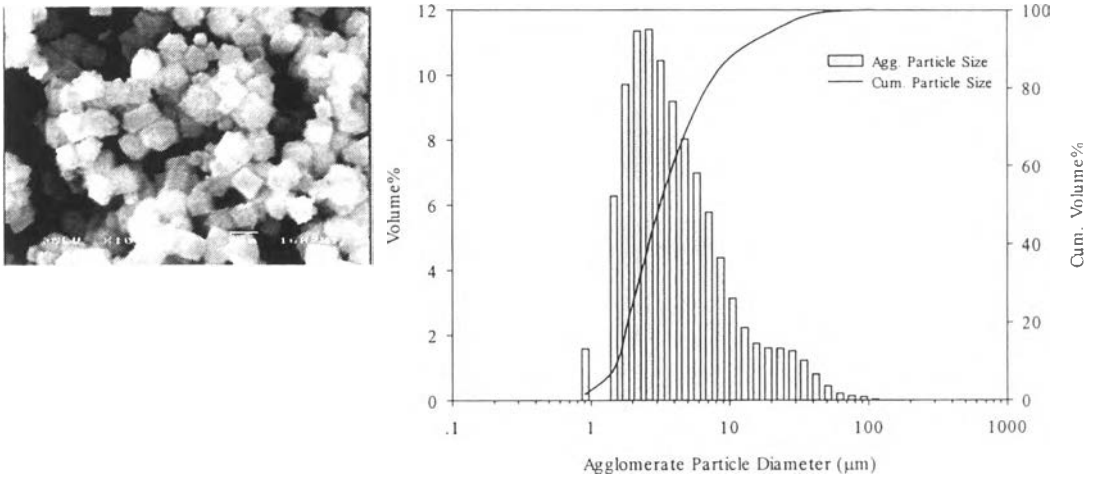

(a)

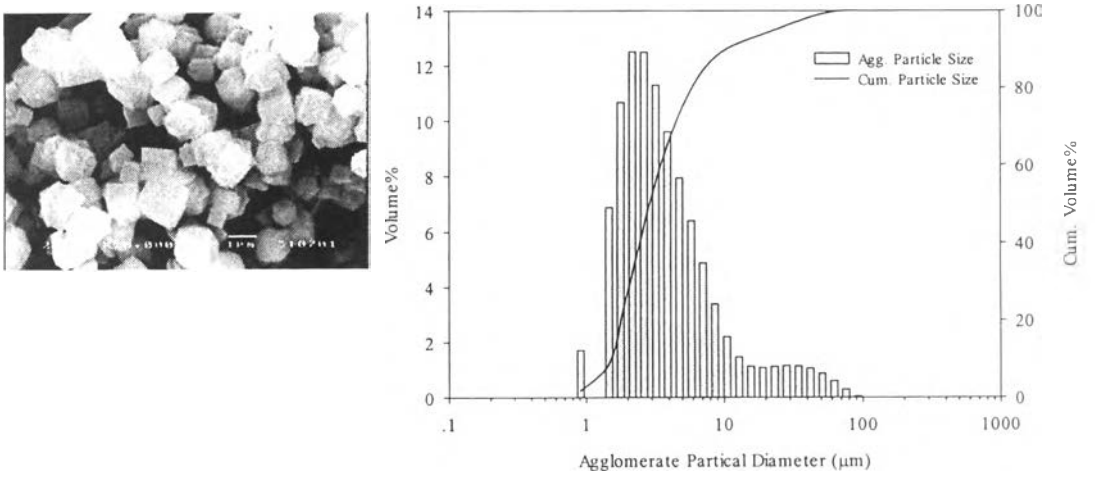

(b)

Figure 3.13 Effect of water quantity on the Na A zeolite synthesized from SiO_2:Al_2O_3: $10Na_2O$:xH_2O (x = 410(a) and 510(b)) and 110°C/5 min

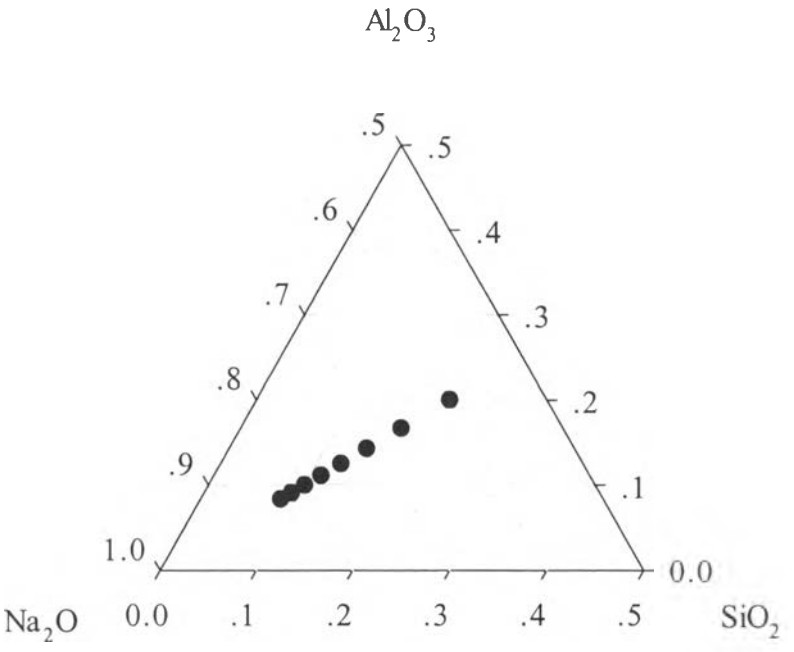

Figure 3.14 Effect of water quantity on the Na A zeolite synthesized from SiO_2:Al_2O_3: $10Na_2O$:xH_2O (x = 410(a) and 510(b)) and 110°C/5 min